Available online at www.sciencedirect.com
SCIENCE DIRECT®
Microelectronic Engineering 77 (2005) 27–35
MICROELECTRONIC ENGINEERING
www.elsevier.com/locate/mee

High performance resist for EUV lithography

K.E. Gonsalves [a,*], M. Thiyagarajan [a], J.H. Choi [a], Paul Zimmerman [b], F. Cerrina [c], P. Nealey [c], V. Golovkina [c], J. Wallace [c], Nikola Batina [d]

[a] *Polymer Chemistry NanoTechnology Laboratory, Department of Chemistry & Cameron Applied Research Center, University of North Carolina, 9201 University City Blvd., Charlotte, NC 28223, USA*
[b] *International SEMATECH2706 Montopolis Drive, Austin, TX 78741, USA*
[c] *Center for Nanotechnology, University of Wisconsin-Madison, Kegonsa Research Campus 3731, Schneider Drive, Stoughton, WI 53589, USA*
[d] *Laboratorio de Nanotecnologia e Ingenieria Molecular, Departamento de Quimica, Area de Electroquimica, Universidad Autonoma Metropolitana-Iztapalapa, Av. San Rafael Atlixco No. 186, Col.Vicentina, 09340 Mexico DF, Mexico*

Received 27 July 2004; accepted 18 August 2004
Available online 11 September 2004

Abstract

As the semiconductor industry moves to the 32 nm node, it becomes apparent that new lithography technology will be needed. One possibility for fabricating this feature size is extreme ultraviolet (EUV) technology. With the advent of EUV, new high performance resist materials will need to be developed. This study looks at the use of a poly[4-hydroxystyrene-*co*-2-(4-methoxybutyl)-2-adamantyl methacrylate] system as a possible candidate material for extreme ultraviolet lithography (EUVL). This material was synthesized and evaluated as an EUV chemically amplified resist. This resist system showed reasonable sensitivity and contrast compared to conventional PMMA resist. This resist system exhibits both negative and positive tone behavior at high and low dose, respectively. A negative pattern of 35 nm L/S (70 nm pitch) was printed using the transmission-grating EUV Interference Lithography (EUV-IL) tool [J.K. Chen, F.H. Ko, H.L. Chen, F.C. Chang, Jpn. J. Appl. Phys. 42 (2003) 3838]. A positive pattern of 50 nm (pitch 180 nm) was achieved using the EUVL tool at Sandia National Laboratory [Synchrotron Radiation Center website www.src.wisc.edu & Center for Nanotechnology website www.nanotech.wisc.edu]. Resist patterns were characterized in detail using scanning electron microscopy and atomic force microscopy. Both showed similar characteristics of the pattern lines.

Keywords: EUV; Lithography; Resist; Adamantyl methacrylate; Hydroxystyrene

* Corresponding author. Tel.: +1 704 687 3501; fax: +1 704 687 6106.
E-mail address: kegonsal@email.uncc.edu (K.E. Gonsalves).
URL: http://www.chem.uncc.edu/faculty/gonsalves/profile_Gonsalves.html.

0167-9317/$ - see front matter
doi:10.1016/j.mee.2004.08.003

1. Introduction

Extreme ultraviolet lithography (EUVL) has evolved into a possible candidate for the mass production of future integrated circuits at the 45 or 32 nm node [1]. Much of the work to date in EUVL has focused on aspects of lithography tool development and has downplayed resist performance. However, the advent of several micro exposure tool over the next year has ignited an interest in developing an EUV resist meeting strict tool and performance requirements. For example, the developed resist must possess reasonable photospeed while maintaining a low level of outgassing components [2]. Another factor that has to be considered is the absorption coefficient of resist materials in the EUV. All materials have high absorption coefficients at 13 nm wavelength due to high atomic ionization cross-section [3]. The presence of aromatic rings may reduce the absorption at 13 nm and also improve the etch resistance of a polymer. So KrF resists based on poly(4-hydroxystyrene) are promising candidates for ultra-thin single layer resist materials for EUVL [3,4]. Besides low absorption and etch resistance as mentioned above, EUV resist materials must have high sensitivity, good adhesion, low out-gassing, and low line edge roughness [1,4]. Highly sensitive EUV resists with enhanced high-resolution capabilities need to be developed. Resolution and sensitivity can be improved by using thin resist films but result in a lowered etch resistance. PMMA and poly(4-hydroxystyrene) based resists are generally used in EUV lithography with various protective groups (acetals, *tert*-butoxycarbonyl, *tert*-butyl, etc.), but these protective groups have poor etch resistance due to their aliphatic structures. Incorporating the acid-cleavable alicyclic substituents such as 2-methyl-2-adamantyl groups into the base polymer can overcome this problem.

Here we propose a hydroxystyrene-based resist with a derivative of adamantyl methacrylate in order to enhance the resolution, sensitivity, and dry etching resistance. The synthesis, physical properties, and basic lithographic performance of the newly designed polymer are described. In order to characterize the lithography patterns and surface morphology of the resist film in detail, AFM analysis was employed. Similar to SEM, AFM is a very useful method to determine the pattern size and the resist film roughness. In addition AFM allows 3D analysis of lithography patterns [5–7].

2. Experimental

2.1. Materials

Acetoxystyrene (DuPont) and 2-(4-methoxybutyl)-2-adamantyl methacrylate (ENF Tech.) were distilled prior to use. 2,2′-Azobisisobutyronitrile (AIBN) was purchased from Aldrich Chemical Company and purified by recrystallization from methanol. Triphenylsulfonium nonafluoro-1-butanesulfonate (TPSNf) as a photoacid generator (PAG) was supplied by Seoul Fine Tech.

2.2. Polymerization

Polymers were prepared by free radical polymerization in sealed pressure vessels. 4-Acetoxystyrene (AcOSty), 2-(4-methoxybutyl)-2-adamantyl methacrylate (MBAMA), and 2,2′-azobisisobutyronitrile (AIBN) as an initiator were dissolved in freshly dried tetrahydrofuran (THF). Polymerization was performed at 65 °C for 24 h and precipitated into a large amount of methanol and dried at reduced pressure. Poly(AcOSty-co-MBAMA) was obtained as a white powder. Poly(4-hydroxystyrene-co-2-(4-methoxybutyl)-2-adamantyl methacrylate), Poly(HOST-co-MBAMA), was then obtained by dispersing poly(AcOSty-co-MBAMA) copolymer in a mixture of ammonium hydroxide and methanol for 6 h. After the dissolution, the mixture was acidified with concentrated acetic acid, and then precipitated into a large volume of distilled water. The precipitate was filtered and then dried at reduced pressure [8].

2.2.1. Poly(AcOSty-co-MBAMA)

^{1}H NMR ($CDCl_3$, ppm): 6.2–7.2 (Phenyl); 3.2–3.4 (CH_3O–); 2.0–2.4 (CH_3COO–); 0–2.0 (Alkyl).

FT-IR (NaCl, cm^{-1}): 3034 (aromatic C=C); 2921 and 2854 (Aliphatic CH), 1766 (CH_3COO–); 1712 (Methacrylate COO–).

2.2.2. Poly(HOSty-co-MBAMA)

NMR (DMSO-d_6, ppm)^{1}H NMR ($CDCl_3$, ppm): 8.8–9.3 (Phenolic **OH**); 6.0–7.0 (Phenyl); 3.0–3.5 (C**H**$_3$O–); 0–2.5 (Alkyl).

FT-IR (NaCl, cm^{-1}): 3384 (Phenolic OH), 2920 and 2861 (Aliphatic CH); 1708 (Methacrylate COO–).

2.3. Lithographic evaluation

Resist solutions were prepared by dissolving 1.0 g of the polymer, 0.05 g of TPSNf, and 0.0025 g of tetrabutylammonium hydroxide in 10.0 g of cyclohexanone. The solution was filtered prior to application on the silicon substrate. A film was prepared by spin coating the resist solution on a silicon wafer and baking at 100 °C for 90 s. The thickness of the film measured using ellipsometer was 135 nm. EUV exposures were conducted at the Synchrotron Radiation Center (SRC) and Center for NanoTechnology (CNTech) [9] and Sandia National Laboratory (10 × Microstepper) [10]. Details of the exposure tool have been provided earlier [11,12]. The exposed wafer was baked again at 120 °C for 90 s and developed by dipping in a conventional 2.38 wt% tetramethylammonium hydroxide (TMAH) developer for 60 s and rinsed with de-ionized water.

2.4. Surface metrology-atomic force microscopy

The surface characterization of the resist film and lithography patterns was performed using a commercial atomic force microscopy (AFM) (Digital Instruments, USA). Images were recorded at ambient conditions, operating the AFM in the "tapping" mode [13]. This method provides less contact between the AFM tip and the sample, which is important in the imaging of soft materials. Along these same lines, images were recorded at a frequency below 1 Hz. Imaging was carried out using standard silicon TESP probes (Digital Instruments), with a 125 μm long cantilever and resonant frequency range between 309 and 382 kHz. The spring constant of the tip was in the range of 20–100 N/m. The shape of the tips used has a direct impact on the images obtained in this work. The tip had a nominal radius between 5 and 10 nm, with cone half angle: 17° side, 25° front and 10 back. As will be discussed later, the tip characteristics impact the feature appearance in the images obtained.

3. Results and discussion

3.1. Synthesis of polymers

Poly(AcOSty-co-MBAMA) with various molar feed ratios were obtained using AIBN as a radical initiator and the polymerization results are summarized in Table 1. Poly(HOSty-co-MBAMA) was made by hydrolysis with ammonium hydroxide in methanol. The overall synthesis is depicted in Scheme 1. After hydrolysis, the formation of hydroxystyrene in the copolymer was confirmed spectroscopically by NMR and IR spectra (Figs. 1 and 2). In the ^{1}H NMR spectrum, the acetyl proton resonance at 2.2 ppm (Fig. 1(a)) completely disappeared

Table 1
Polymerization results of poly(HOSty-co-MBAMA)

Polymer	Molar feed ratio (mol%)		Copolymer composition[a] (mol%)		Yield (%)	M_w (MWD)[b]	T_g[c] (°C)
	AcOSty	MBAMA	HOST	MBAMA			
1	90	10	87	13	71	3290/3.1	157
2*	82	18	81	19	66	2046/2.1	145
3	70	30	73	27	57	2245/2.1	143

[a] Copolymer compositions were calculated by ^{1}H NMR spectrum.
[b] M_w and MWD were calculated with polystyrene standards.
[c] The glass transition temperatures (T_g) were measured at a heating rate 10 °C/min.
* Indicates sample used for imaging.

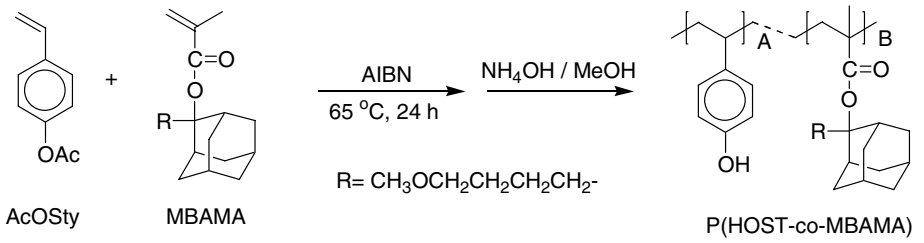

Scheme 1. Synthesis of polymers.

after hydrolysis (Fig. 1(b)). The resonance peak at 9.1 ppm (Fig. 1(b)) was assigned to the hydroxyl proton resonance, which confirmed the formation of hydroxystyrene. The resonance peaks in the region of 6.2–7.2 were assigned to phenyl protons. The methoxy proton resonance appears at 3.3. The aliphatic methyl, methylene and methine proton resonances appear at around 0.8–2.5 ppm. In the FT-IR spectrum, a broad –OH stretching band appeared around 3300 cm^{-1}, corresponding to the phenolic OH group present in poly(hydroxy styrene). Further confirming the formation of the hydroxy styrene, was the absence of the carbonyl stretching band at 1766 cm^{-1}. The weight average molecular weight (M_w) of the polymers (Table 1) ranged from 2000 to 3300. The M_w of sample 2 was 2046 with a polydispersity of 2.1 used for imaging. The glass transition temperature (T_g) of poly (HOST-co-MBAMA) is around 145 °C.

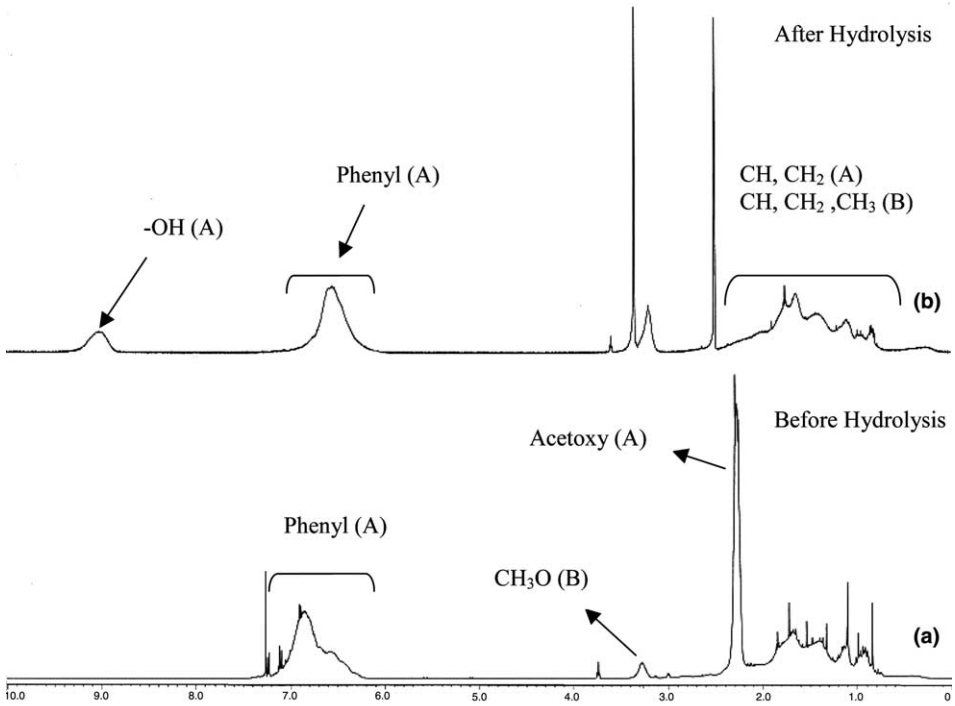

Fig. 1. 500 MHz ^{1}H NMR spectra of: (a) poly(AcOSty-co-MBAMA) in $CDCl_3$; (b) poly(HOST-co-MBAMA) in DMSO-d_6.

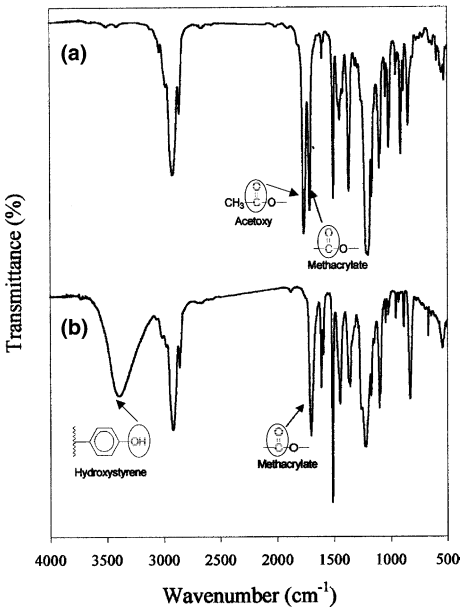

Fig. 2. FT-IR spectra of poly(HOST-co-MBAMA): (a) before hydrolysis; (b) after hydrolysis.

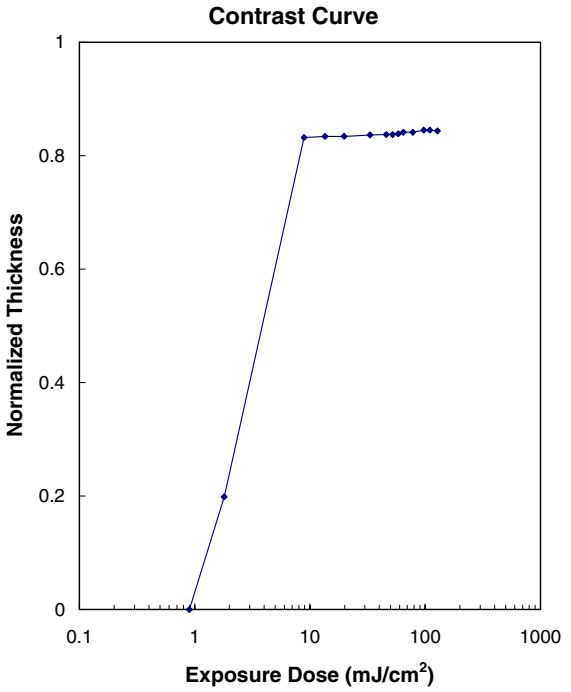

Fig. 3. Contrast curve of negative resist sample formulated with poly(Host-co-MBAMA).

3.2. Lithographic evaluation

In many aspects, EUVL may be viewed as an extension of optical lithography since it uses short wavelength (13.4 nm) radiation to carry out projection imaging. In spite of this similarity, there are major differences between the two technologies. Most of these differences occur because the properties of the materials in the EUV portion of electromagnetic spectrum are different from those in the visible and UV wavelengths ranges. In order to keep pace with the demand for the printing of smaller features, it is necessary to gradually reduce the wavelength of the light used for imaging and to design imaging systems with larger numerical apertures [14,15]. EUV lithographic evaluation was performed on the EUV beam line at University of Wisconsin-Madison [9] and Sandia National Laboratory [10]. Sensitivity and contrast values were calculated based on the normalized thickness (NRT) curves for these resist systems formulated with polymer poly(HOST-co-MBAMA) (Fig. 3). This resist showed negative tone at high dose. Though this resist system was originally designed as a positive system, yet it showed a negative type contrast curve as reported earlier for analogous systems [16–20]. In ESCAP and PHOST resists, negative tone behavior at higher doses has been observed previously for EUV [21–23].

The resist exhibited a sensitivity of 9 mJ/cm^2 and contrast of 2.0 as a negative system for EUV exposure using a conventional 2.38 wt% TMAH developer. The sensitivity and contrast values were reasonably good compared to conventional PMMA resist [9]. The clearing was 9 mJ/cm^2 for negative tone and 5.2 mJ/cm^2 for positive tone. There was about 20% thickness loss of the unexposed area of the patterned surface after development, which was attributed to the low molecular weight of the initial polymer (M_w 2046). It is anticipated that increasing the molecular weight to >3500 will result is eliminating any dark loss.

The scanning electron micrograph of the line and space patterns for the resist formulated with poly (HOST-co-MBAMA) is shown in Fig. 4. The negative pattern of 35 nm L/S (70 nm pitch) was printed using transmission-grating EUV

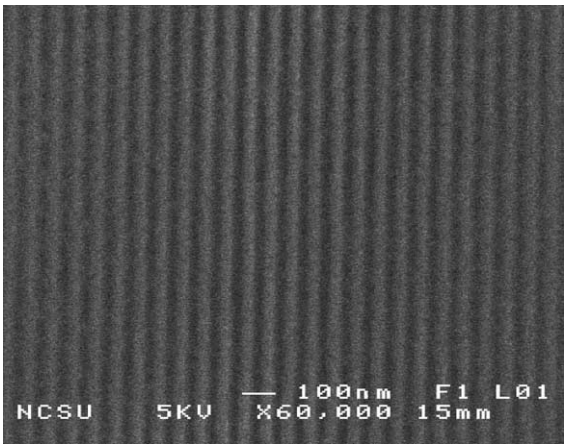

Fig. 4. Scanning electron micrograph of negative resist, poly(HOST-co-MBAMA).

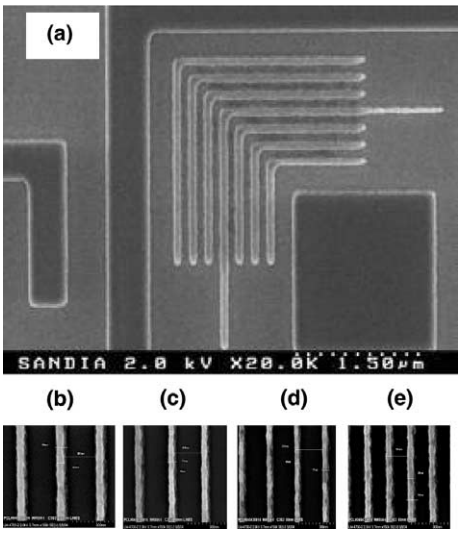

Fig. 5. Extreme UV lithography pattern profiles of positive resist poly(HOST-co-MBAMA): (a) 100 nm line and space (1:1) elbow pattern; (b)–(e) 100–50 nm line (pitch 180 nm) pattern.

Interference Lithography (EUV-IL) tool [24]. Depending on the electron beam current in the storage ring, typical exposure time never exceeded 140 s.

The scanning electron micrographs of positive tone patterns for the resist are shown in Fig. 5. The resist patterns of 100 nm elbow (Fig. 5(a)) and 100 (302 nm pitch), 90 (270 nm pitch), 80 (237 nm pitch) and 60 nm (180 nm pitch) lines (Fig. 5(b)) were obtained at a dose of 10.4 mJ/cm^2 It should be mentioned that during the exposures a small amount of base(tetra butyl ammonium hydroxide) was used in order to control acid diffusion effects [25].

3.3. Metrology-AFM analysis

The use of AFM provides a capability for direct and quantitative observation of the resist profiles. Nanometer scale line edge roughness and surface roughness are increasingly important factors in critical dimension control as the minimum feature sizes of devices continue to shrink.

Fig. 6 represents the AFM surface image (5×5 μm) of polymer 2, with a clearly developed lithographic pattern (Fig. 6(a)). The width of the lines was found to be between 45 and 60 nm. The depth profile analysis shows that the lithographic patterns possess a depth of only 1–1.5 nm. In the case of soft material, AFM imaging is very much affected by magnitude of the tip-sample interactions and the shape of the AFM tip. Although the less disturbing ''tapping'' mode was used for image recording, it was noticed that image quality was very sensitive to the magnitude of the force applied to the sample. Additionally, the observed shallow depth of the lithographic lines could be the result of the specific geometry of the AFM tips used. This geometry may have prevented the tips from reaching the bottom of the patterned lines. Note that the tip has a pyramidal shape 10–15 μm long with apex between 5 and 10 nm and angles of 10°, 17° and 25°. These dimensions could lead to difficulties in reaching the bottom of the trenches. It is anticipated that the lithographic feature sizes were of the same order of magnitude as the AFM tip, and hence depth of profiling is likely not to be determined exactly. Obviously to resolve this problem, in the future, ultra sharp AFM tips with much higher aspect ratio must be used [26,27].

High resolution AFM image of the polymer surface (0.44×0.44 μm) presented in Fig. 6(b) shows details regarding the surface characteristics of the patterned sample. In particular the surface characteristics of the polymer surface left

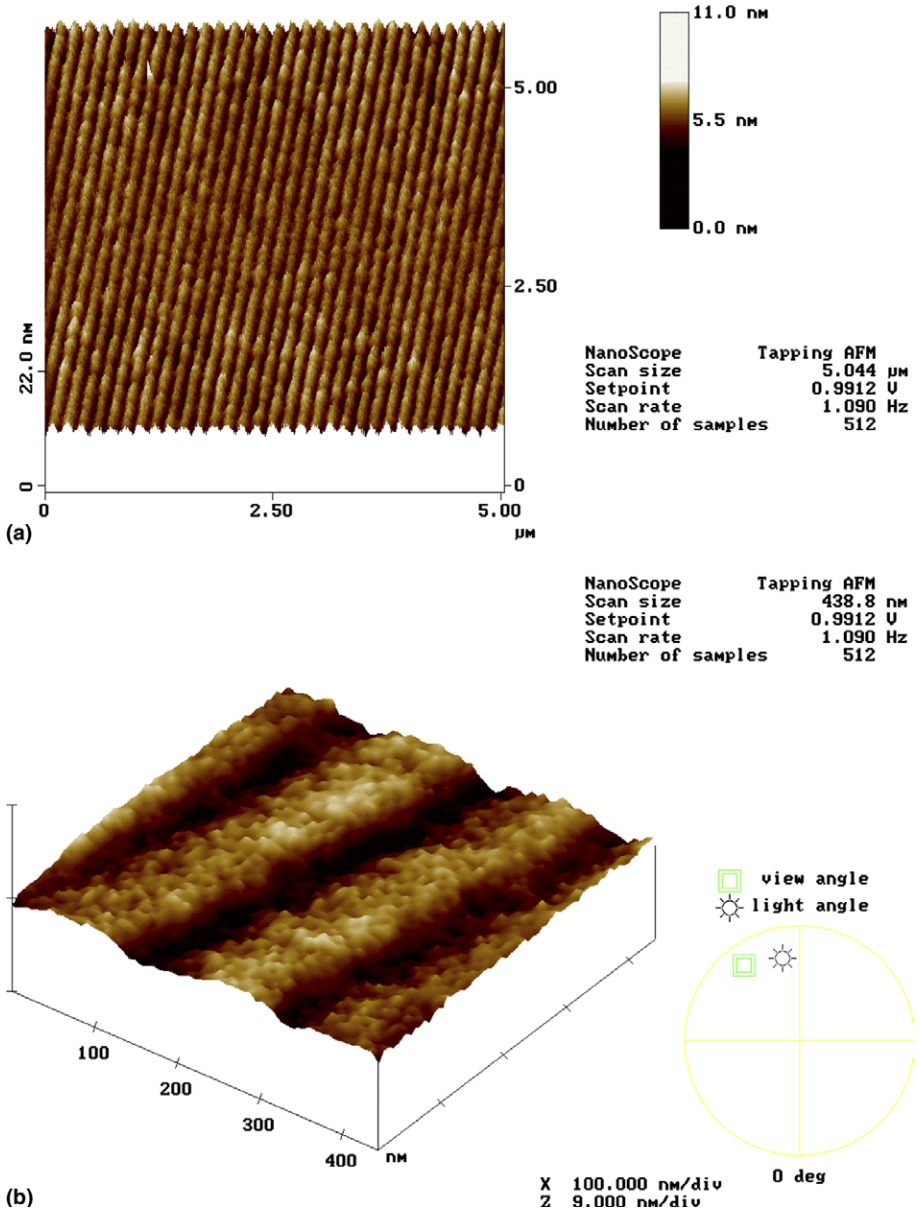

Fig. 6. AFM Images of negative resist poly(HOST-co-MBAMA): (a) 5×5 μm; (b) 0.4×0.4 μm.

between pattern lines could be observed. It is obvious that the polymer surface is not flat. It consists of nodular features with diameter between 5 and 7 nm. They are randomly distributed on the surface at different levels in the range of 0.3–0.5 nm. Note that z scale (image height) for the whole image including the patterned lines is only 9 nm/division. The surface roughness estimated for this part of the sample surface RMS[Rq] = 0.169 nm. Such topography is indicative of an inhomogeneously dissolved pattern profile. Further it has been observed that the surface roughness and sidewall roughness of the resist patterns can also be directly attributed to the resist contrast as well as polymer dissolution characteristics [28,29]. This may indicate

that lower contrast resists create regions near the mask edge, gradually changing distributions of soluble and insoluble polymer molecules. This condition is known to lead to percolative dissolution behavior characterized by developer channel, swelling and rough line edges [30]. At a high dissolution rate, the effect of thickness loss clearly dominates over other potential contributions to the roughness. Low molecular weight polymers consistently have higher dissolution rates and produce resists with higher film thickness loss [31]. The molecular weight of Poly (HOST-co-MBAMA) used in this study was quite low (~2000) and the resist formulated with this copolymer showed high film thickness loss (~20%) after development.

4. Conclusion

The bulky protective group, 2-(4-methoxybutyl)-2-adamantyl group, was introduced into the matrix polymer in order to improve sensitivity, resolution, and etch resistance. The resists formulated with poly(HOST-co-MBAMA) showed reasonable sensitivity and contrast compared to conventional PMMA resist. The resist formulated with poly(HOST-co-MBAMA) gave 35 nm line patterns with EUV lithography. Unexpectedly, this resist behaved as a negative resist in the EUV even though it showed behavior as a conventional positive resist at low dose. Additional studies to eliminate the dark-loss and optimize photospeed are underway. Further detailed investigation on correlation of reactivity ratios and composition heterogeneity of the polymer resist is in progress.

Acknowledgements

We acknowledge International SEMATECH for funding (Project CT # LITK101). This work was performed using the EUV beamline and research facilities at the Center for NanoTechnology at the University of Wisconsin-Madison and Sandia National Laboratory. Professor N. Batina is grateful for the support of UAM-I and Instituto Mexicano de Petroleo (IMP, project FIES 98-100-I). We acknowledge Professor Cliff Henderson and Dr. A. Jeyakumar at the School of Chemical and Biomolecular engineering at Georgia Institute of Technology for refractive index measurements. We thank DuPont Electronic Technology USA and ENF Technology Korea for the supply of specialty chemicals.

References

[1] R.L. Brainard, J. Cobb, C.A. Cutler, J. Photopolym. Sci. Technol. 16 (3) (2003) 401.
[2] P.M. Dentinger, L.L. Hunter, D.J. O'Connell, S. Gunn, D. Goods, T.H. Fedynyshyn, R.B. Goodman, D.K. Astolfi, J. Vac. Sci. Technol. B 20 (6) (2002) 2962.
[3] N.N. Matsuzawa, S. Okazaki, A. Ishitani, Microlithography World, Autumn (2000) 20.
[4] R.L. Brainard, C. Henderson, J. Cobb, V. Rao, J.F. Mackevich, U. Okoroanyanwu, S. Gunn, J. Chambers, S. Connolly, J. Vac. Sci. Technol. B 17 (6) (1999) 3384.
[5] K.E. Gonsalves, W. He, N. Batina, D.B. Poker, L.Merhari, in: L. Merhari, K.E. Gonsalves, E.A. Dobisz, M. Angelopoulos, D. Herr (Eds.), Proceedings of the 2001 MRS Fall Meeting, Symposium "Nanopatterning-From Ultralarge Scale Integration to Biotechnology", Mat. Res. Soc. Symp. Proc., vol. 705, 2002, pp. Y4.6.1–Y4.6.6.
[6] W. He, D.B. Poker, K.E. Gonsalves, N. Batina, Microelectron. Eng. 65 (1–2) (2003) 153.
[7] W. He, K.E. Gonsalves, N. Batina, D.B. Poker, E. Alexander, M. Hudson, Biomed. Microdev. 5 (2) (2003) 101.
[8] H. Ito, G. Breyta, D. Hofer, R. Sooriyakumaran, J. Photopolym. Sci. Technol. 7 (3) (1994) 433.
[9] Synchrotron Radiation Center website www.src.wisc.edu & Center for Nanotechnology website www.nanotech.wisc.edu.
[10] Sandia National Laboratories at www.sandia.gov.
[11] M.A. Ali, V. Golovkina, F. Cerrina, K. Gonsalves, Microelectron. Eng. 65 (4) (2003) 454.
[12] M.A. Ali, N. Batina, V. Golovkina, F. Cerrina, K. Gonsalves, Proc. SPIE 5039 (Part 2) (2003) 1173.
[13] Scanning Probe Microscopy Training Notebook, Digital Instruments, Santa Barbara, USA, 1996.
[14] T.E. Jewell, J.M. Rodgers, K.P. Thompson, J. Vac. Sci. Technol. B8 (1990) 1509.
[15] G.E. Sommargren, Laser Focus World 32 (1996) 61.
[16] S.G. Hansen, V. Dommelen, Youri, Proc. SPIE 4404 (2001) 80–88.
[17] T. Evangelia, G. Evangelos, A. Panagiotis, R. Ioannis, G.P. Patsis, G. Nikos, C.H. Tan, Zoilo, K.Y. Lee, P.T. Le, Y. Hsu, H. Michael, Proc. SPIE 3999 (2000) 1181–1188.

[18] T. Tada, T. Kanayama, A.P.G. Robinson, R.E. Palmer, M.T. Allen, J.A. Preece, K.D.M. Harris, Microelectron. Eng. 53 (2000) 425–428.
[19] A.P.G. Robinson, R.E. Palmer, T. Tada, T. Kanayama, M.T. Allen, J.A. Preece, K.D.M. Harris, J. Phys. D: Appl. Phys. 32 (1999) L75–L78.
[20] Dan V. Nicolau, Takahisa Taguchi, Hiroshi Taniguchi, Susumu Yoshikawa, Langmuir 15 (1999) 3845–3851.
[21] W. Domke, S. Hirscher, O. Kirch, K. Kragler, K. Lowack, in: Second International EUVL Symposium, Antwerp, Belgium, 2003.
[22] J.K. Chen, F.H. Ko, H.L. Chen, F.C. Chang, Jpn. J. Appl. Phys. 42 (2003) 3838.
[23] J.O. Choi, J.A. Moore, J.C. Moore, J.C. Corelli, J.P. Silverman, H. Bakhru, J. Vac. Sci. Technol. B6 (1988) 2286.
[24] V.N. Golovkina, P.F. Nealey, F. Cerrina, J.W. Taylor, H.H. Solak, C. David, J. Gobrecht, J. Vac. Sci. Technol. B22 (2004) 99.
[25] Y. Toshiyuki, S. Hiroshi, T. Tsuneo, O. Shinji, J. Vac. Sci. Technol. B: Microelectron. Nano. Struct. 14 (6) (1996) 4216.
[26] N.G Orji, M.I. Sachez, J. Raja, T.V. Vorburger, AFM characterization of semiconductor line edge roughness, in: Bhushan, Fuchs, Hosaka (Eds.), Applied Scanning Probe Methods, Springer-Verlag, Berlin, 2004.
[27] M. Bishop, D. McCormack, J.S. Villarrubia, N.G. Orji, J.A. Allgair, Proc. SPIE 5375 (2004) 515–533.
[28] M. Budhlall, O.L. Shaffer, E.D. Sudol, V.L. Dimonie, M.S. El-Aasser, Langmuir 19 (2003) 9968B–9972B.
[29] R.L. Brainard, C. Henderson, J. Cobb, V. Rao, J.F. Mackevich, U. Okoroanyanwu, S. Gunn, J. Chambers, S. Connolly, J. Vac. Sci. Technol. B 17 (6) (1999) 3384.
[30] R.L. Brainard, J. Cobb, C.A. Cutler, J. Photopolym. Sci. Technol. 16 (3) (2003) 401.
[31] H.J. Butt, R. Kuropka, B. Christensen, Coll. Polym. Sci. 272 (1994) 1218.